Wireless Power Transfer—An Overview

Zhen Zhang, *Senior Member, IEEE*, Hongliang Pang, *Student Member, IEEE*, Apostolos Georgiadis, *Senior Member, IEEE*, and Carlo Cecati, *Fellow, IEEE*

(Invited Paper)

***Abstract*—Due to limitations of low power density, high cost, heavy weight, etc., the development and application of battery-powered devices are facing with unprecedented technical challenges. As a novel pattern of energization, the wireless power transfer (WPT) offers a band new way to the energy acquisition for electric-driven devices, thus alleviating the over-dependence on the battery. This paper presents an overview of WPT techniques with emphasis on working mechanisms, technical challenges, metamaterials, and classical applications. Focusing on WPT systems, this paper elaborates on current major research topics and discusses about future development trends. This novel energy transmission mechanism shows significant meanings on the pervasive application of renewable energies in our daily life.**

***Index Terms*—Capacitive coupled power transfer (CCPT), contactless charging, dynamic charging, inductive power transfer (IPT), overview, wireless power transfer (WPT).**

I. Introduction

As an epoch-making technique, wireless power transfer (WPT) incredibly realizes the energy migration in a cordless way [1], [2]. This seemingly magic way can change our traditional utilization patterns of the energy in various applications, such as portable electronic devices, implanted medical devices, integrated circuits, solar-powered satellites, electric vehicles (EVs), unmanned aerial vehicles (UAVs), and so forth. By means of its remarkable characteristics of flexibility, position-free, and movability, the WPT technique has been taken as an ideal technical solution for energizing electric-driven devices within some specific regions in the near future, especially for smart home applications.

Manuscript received January 11, 2018; revised March 20, 2018; accepted April 24, 2018. Date of publication May 10, 2018; date of current version September 28, 2018. This work was supported in part by the National Natural Science Foundation of China under Project 51607120, in part by the Natural Science Foundation of Tianjin China under Project 16JCQNJC01500, in part by Tianjin University, Tianjin, China, through the PEIYANG Scholar-Reserved Academic Program under Project 2017XRX-0017, and in part by Project MISE-PON n. F/050220/01-02-03/X32. *(Corresponding author: Zhen Zhang.)*

Z. Zhang and H. Pang are with the School of Electrical and Information Engineering, Tianjin University, Tianjin 300000, China (e-mail: zhangz@eee.hku.hk; superphl@tju.edu.cn).

A. Georgiadis is with the 3120 Heriot-Watt University, EH14 4AS Edinburgh, U.K. (e-mail: a.georgiadis@hw.ac.uk).

C. Cecati is with the DISIM, University of L'Aquila, 67100 L'Aquila, Italy, and also with DigiPower srl (e-mail: carlo.cecati@univaq.it).

Color versions of one or more of the figures in this paper are available online at http://ieeexplore.ieee.org.

Digital Object Identifier 10.1109/TIE.2018.2835378

The reason why WPT technologies are so crucial is regarding to two fundamental problems of battery-powered devices that limit their popularization—short battery life and high initial cost. Taking EVs as an example [3], although many automobile manufacturers claim that their products can run over 120 km per charge, when taking into account the range anxiety, most of the EV drivers only dare to run about 100 km. On the other hand, by significantly increasing the number of batteries installed in EVs, the driving range can be extended to over 400 km but the corresponding initial cost becomes unaffordable for the general public. Instead of waiting for the breakthrough of energy storage technology, a new energization way, namely the WPT technique, is attracting increasing attentions to bypass the current technical bottlenecks of batteries. By utilizing the WPT technique, battery-powered devices can harness wireless power from electromagnetic field in air and then charge their batteries cordlessly even in the moving state. This novel charging technology can fundamentally solve their problems of short battery life due to limited battery storage or high initial cost due to the installation of a large number of batteries.

The rest of this paper is organized as follows. Section II will elaborate the working mechanism of inductive power transfer (IPT), capacitive compensation network, magnetic resonant coupling, and capacitive coupled power transfer (CCPT). In Section III, this paper will systematically summarize major technical challenges, such as the efficiency, power, distance, misalignment, omnidirectional charging, and security. Section IV will discuss about the metamaterials and its improvement on the transmission performance of WPT systems. Section V introduces classic WPT applications, including EVs, implantable biomedical devices, and portable electronic devices. Finally, Section VI will draw conclusions and discuss about future prospects for WPT systems.

II. Fundamentals

The WPT technique has an ability of delivering the energy from the power supply to the target via the air instead of traditional wires. This novel energy accessing technique commonly consists of the far-field and the near-field transmissions. The far-field WPT can be realized by adopting the acoustic, the optical, and the microwave as the energy carrier. The near-field technique utilizes the inductive coupling effect of nonradiative electromagnetic fields, including the inductive and capacitive mechanisms, which is exactly the emphasis of this paper.

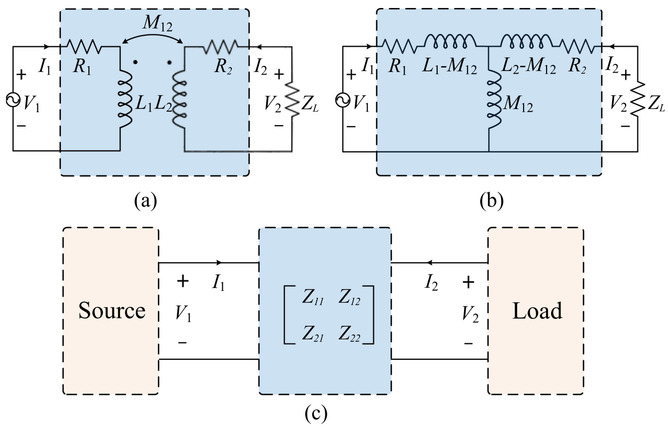

Fig. 1. IPT. (a) Circuit model. (b) Equivalent T-model. (c) Two-port network model.

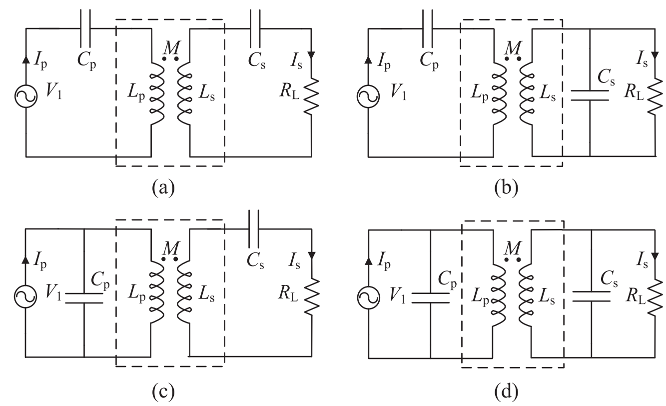

Fig. 2. Compensation networks.

A. Inductive Power Transfer (IPT)

Fig. 1(a) depicts the circuit model of IPT systems [4], [5], where the transmitting coil L_1 and the receiving coil L_2 are directly connected to the power source and the load impedance Z_L, respectively. Denote M_{12} as the mutual inductance, R_1 and R_2 as the equivalent ac resistance of coils. According to the T-model as shown in Fig. 1(b) and the two-port network model as shown in Fig. 1(c), the voltage equation can be obtained as

$$\begin{bmatrix} V_1 \\ V_2 \end{bmatrix} = \begin{bmatrix} Z_{11} & Z_{12} \\ Z_{21} & Z_{22} \end{bmatrix} \begin{bmatrix} I_1 \\ I_2 \end{bmatrix} = \begin{bmatrix} R_1 + j\omega L_1 & j\omega M \\ j\omega M & R_2 + j\omega L_2 \end{bmatrix} \begin{bmatrix} I_1 \\ I_2 \end{bmatrix}. \quad (1)$$

The corresponding input and output impedances can be calculated as

$$\begin{cases} Z_{\text{in}} = Z_{11} - \frac{Z_{12}^2}{Z_{22}+Z_L} \\ Z_{\text{out}} = Z_{22} - \frac{Z_{12}^2}{Z_{11}+Z_S} \end{cases}. \quad (2)$$

By neglecting resistive losses, the power acquired by the load can be given by

$$P_L = \frac{\kappa_{12}^2 L_2 R_L}{L_1} \frac{1}{\left[\omega L_2 \left(1-\kappa_{12}^2\right) + X_L^2\right]^2 + R_L^2} |V_1|^2. \quad (3)$$

Denote the coupling coefficient between the transmitting and the receiving coils as κ_{12}, which is given by

$$\kappa_{12} = \frac{M_{12}}{\sqrt{L_1 L_2}}. \quad (4)$$

Since IPT systems fall into the loosely coupled region ($\kappa_{12} << 1$), the transmitted power can be simplified as

$$P_{L,\kappa \ll 1} \approx \frac{L_2}{L_1} |V_1|^2 \frac{R_L}{\left(\omega L_2 + X_L\right)^2 + R_L^2} \kappa_{12}^2. \quad (5)$$

It shows that the load power is determined by the coupling coefficient κ_{12}. Meanwhile, the model between the distance d and κ_{12} is given by [6]

$$\kappa_{12} = \frac{2r}{\left[\ln(8r/a) - 2\right]\sqrt{d^2+4r^2}} \int_2^{\frac{\pi}{2}} \frac{\left(2\sin^2\phi - 1\right)}{\sqrt{1 - \frac{4r^2 \sin^2\phi}{d^2+4r^2}}} d\phi \quad (6)$$

where r is the radius of coil and a is the cross-sectional radius of copper wire. Accordingly, the load power will dramatically drop with the increasing of the transmission distance d in IPT systems. This is the reason why IPT systems can only deal with the near-field energy transmission.

Additionally, the efficiency η can be calculated as

$$\eta = \frac{P_L}{P_{\text{in}}} = \left| \frac{Z_{12}}{Z_L + Z_{22}} \right|^2 \frac{\mathrm{R}e\left\{Z_L\right\}}{R_1 + \frac{\omega^2 M_{12}^2 (R_2+R_L)}{(R_2+R_L)^2 + (X_2+X_L)^2}}. \quad (7)$$

In order to achieve the maximum η, the optimal load impedance Z_L can be determined by differentiating η with respect to R_L and X_L. It can be given by

$$Z_{L,\text{opt}} = R_2 \sqrt{1 + \kappa_{12}^2 Q_1 Q_2} - j\omega L_2 \quad (8)$$

where Q_1 and Q_2 represent the quality factor of transmitting and receiving coils, respectively. Accordingly, the maximum efficiency is given by

$$\eta_{\max} = \frac{\kappa_{12}^2 Q_1 Q_2}{\left(1 + \sqrt{1 + \kappa_{12}^2 Q_1 Q_2}\right)^2}. \quad (9)$$

By taking into account the loosely coupled effect ($\kappa_{12} << 1$) in IPT systems, the quality factors of coils should be high enough to ensure the expected energy transmission efficiency.

B. Compensation Network

According to (5), it shows that the primary and the secondary circuits both need a capacitive compensation to eliminate the imaginary part [7], aiming to ensure the maximum V_1 and minimum $(\omega L_2 + X_L)^2$. Regarding to the capacitive compensation network, there are four topologies as shown in Fig. 2, namely series–series (SS), series–parallel (SP), parallel–series (PS), and parallel–parallel (PP). By using the reflected impedance theory, the compensated capacitances can be calculated with respect to various network topologies [8], which are listed in Table I. It should be noted that the SS is the only topology which is independent of the coupling coefficient and the load condition since the reflected reactance equals zero on the primary side.

TABLE I
CAPACITIVE COMPENSATION NETWORK

Topology	Secondary quality factor	Reflected resistance	Primary capacitance
SS	$\frac{\omega_0 L_s}{R}$	$\frac{\omega_0^2 M^2}{R}$	$\frac{C_s L_s}{L_p}$
SP	$\frac{R}{\omega_0 L_s}$	$\frac{M^2 R}{L_s^2}$	$\frac{C_s L_s^2}{L_p L_s - M^2}$
PS	$\frac{\omega_0 L_s}{R}$	$\frac{\omega_0^2 M^2}{R}$	$\frac{C_s L_s}{\frac{M^4}{L_p C_s L_s R} + L_p}$
PP	$\frac{R}{\omega_0 L_s}$	$\frac{M^2 R}{L_s^2}$	$\frac{(L_p L_s - M^2) C_s L_s^2}{\frac{M^4 C_s R}{L_s} + (L_p L_s - M^2)^2}$

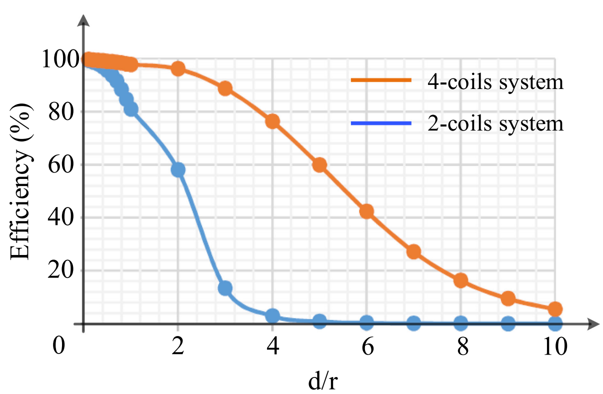

Fig. 3. Difference of impact between the distance on efficiency of two-coils and four-coils IPT systems.

C. Magnetic Resonant Coupling

Fig. 1(b) depicts the equivalent T-model of two-coils IPT systems, the energy efficiency η_2 can be calculated as [9]

$$\eta_2 = \frac{R_2 R_L}{R_2(R_2 + R_L) + \frac{(R_2+R_L)^2}{\kappa_{12}^2 Q_1 Q_2}}. \tag{10}$$

In order to illustrate the impact of d on η_2, this paper takes an exemplification by adopting $r = 30$ cm, $a = 3$ mm, and $Q_1 = Q_2 = 1000$. Fig. 3 illustrates that the efficiency η_2 drops dramatically when $d > 2r$. This is the reason why the two-coils IPT system is commonly used for short-range (shorter than the diameter of the coil) transmission applications.

In order to improve the performance of transmission efficiency, the four-coils IPT system was proposed by utilizing additional sending and receiving coils [10]. Fig. 4 depicts the equivalent T-model of four-coils IPT systems, where C_1, C_2, R_1, and R_2 are the parasitic capacitances and the parasitic resistances of the additional sending and receiving coils. In such ways, the input and the load impedances can be regulated to equal the optimal values as in (8) by adjusting κ_{13} and κ_{24}, which cannot be carried out in the two-coils IPT system. Actually, the additional two coils in the four-coils IPT system are

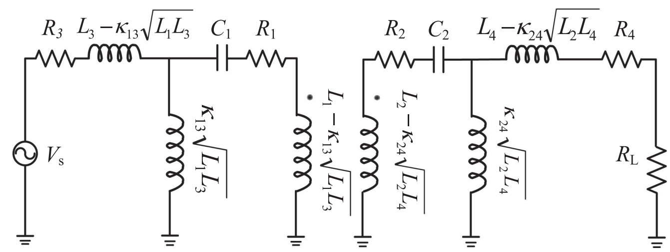

Fig. 4. Equivalent T-model of four-coils IPT systems.

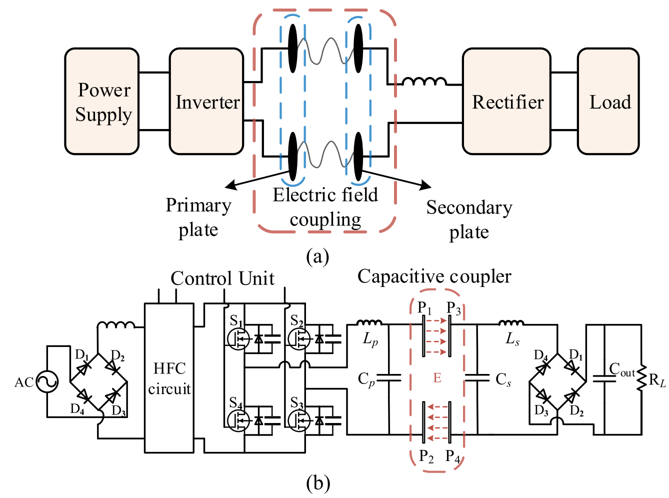

Fig. 5. Typical CCPT system. (a) Block diagram. (b) Circuit.

designed to play the role of impedance matching and this is the reason why the four-coils IPT system can ensure the energy efficiency at a high level even under a weak coupling effect [11], thus extend the transmission distance to the midrange applications. However, immediately the number of coils is increased to four there existing tuning troubles which are not feasible to have the four-coils structure under the circumstances of coplanar situation in the primary side such as EV charging.

D. Capacitive Coupled Power Transfer (CCPT)

The CCPT systems deliver the energy via the electric field instead of the magnetic field; thus, possessing an ability of penetrating through metal materials existing in the transmission path, which is the most different from the IPT systems. Fig. 5 shows the block diagram and the equivalent circuit of the CCPT systems, where the energy can be contactless transmitted through the coupling electric field between the primary and secondary plates. In order to in-depth understand the working mechanism and steady-state performance of the CCPT systems, an accurate nonlinear circuit model was proposed by using the stroboscopic theory in [12]. By means of its potentials to improve the tolerance for transmission mediums and reduce the electromagnetic interference (EMI), a number of attempts have been carried out with emphasis on the power, the efficiency, the communication and EMI as follows.

1) Transmission Power: In [13], for example, four single active switch CCPT topologies were investigated based on the canonical Cuk, SEPIC, Zeta, and Buck–Boost converters, which aim to increase the transmitted power to kilowatt level and remain cost effective. In [14], a portable ceramic dielectric surface was utilized to increase the high power density of CCPT systems. In [15], a comparative study was carried out to reveal the impact of the inductor position on the transmission performance of the CCPT systems.

2) Energy Efficiency: In [16], an autofrequency tuning scheme was developed based on the suboptimal Class-E^2 converter to minimize the switching loss caused by the load variations, which aims to improve the transmission efficiency for the CCPT systems. In [17], a double-sided *LC*-compensation circuit was proposed for long-distance transmission, which can offer both constant-voltage and constant-current working modes as well as improve the transmission efficiency under the loosely coupled effect.

3) EMI and Communication: In [18], a six-plate capacitive coupler was proposed by utilizing two additional plates above and below the conventional four-plate couplers, which can effectively reduce the electric field emissions for the large air-gap CCPT systems. By adopting a full-duplex communication on a shared transmission channel, a wireless power and signal transmission scheme was also realized for the CCPT systems in [19].

Besides, a comparative study was conducted between IPT and CCPT systems in [20], by analyzing the theoretical and empirical limitations, summarizing the differences (including power, distance, frequency and efficiency), and proposing a selection guideline for short-range WPT applications. In addition, the CCPT system was successfully utilized for various applications, such as EVs [21], synchronous electric machines [22], and consumer electronics [23].

III. Challenges

The near-field WPT technique is embracing a high-speed development period in recent years. There are increasing academic researchers and industrial engineers who focus on improving the energy transmission performance with emphasizes on the efficiency, capability, applicability, flexibility, security, and so forth. In this section, this paper will overview key technical challenges for nonradiative electromagnetic WPT systems.

A. Energy Efficiency

The maximum energy efficiency is the most important technical concern for WPT systems. Fig. 6 shows various efficiencies along the transmission path [24]. In order to increase the efficiency, a number of work have been reported in previous studies, which can be classified into the coils design, the circuit topology, and the power control.

1) Coil Design: In order to ensure the high efficiency of WPT systems, the quality factor (Q) is the key to the coil design. In [25], an improved hollow planar spiral winding scheme was proposed to improve the Q by using a nonunity Track-Width-Ratio geometry and increasing the inner radius of the winding. In addition, an intermediate coil was utilized for the WPT system [26], which can boost the apparent self-inductance and magnetizing inductance for the primary unit at around the resonant frequency, thus effectively compensating the apparent coupling coefficient. In [27], a new U-coil WPT system was developed to improve the energy efficiency, ensure the cleanliness of the space along the energy transmission direction, and increase the power density.

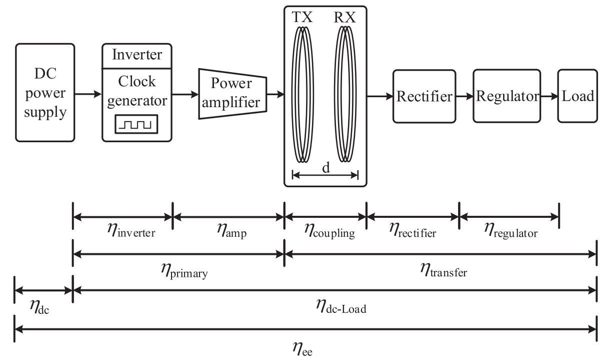

Fig. 6. Efficiency of WPT systems.

2) Circuit Topology: In [28], a series-shunt mixed-resonant coupling topology was presented, which can effectively improve the transmission efficiency as well as the distance. In [29], an active single-phase rectifier was implemented by using an auxiliary measurement coil, which can regulate the equivalent load impedance and the output voltage. Based on the exemplified 800-W prototype, the efficiency can be increased by 2% and 10% for the rated load and the light load, respectively. Besides, the frequencies can be identified for the maximum efficiency and the load-independent voltage-transfer ratio based on the SS and SP compensation networks [30], respectively, which is conductive to realize the efficient power conversion.

3) Power Control: In order to emulate the optimal load value, the switched-mode converter was adopted in the receiving unit and controlled based on the minimum input power operating point [31]. By controlling the amplitude of the output voltage and the phase shift of the active rectifier, the equivalent load impedance can be modified to maximize the energy transmission efficiency [32]. In [33], by using an efficiency evaluation scheme for the closed-loop WPT system, a maximum efficiency point tracking control scheme was proposed to maximize the energy efficiency when regulating output voltage with respect to the varying load and coupling effect. In addition, a series resonant tank was also effective to ensure the maximum efficiency tracking while regulating the output voltage [34]. Regarding to various loads, a cascaded boost–buck dc–dc converter was designed to ensure the optimal impedance matching for WPT systems [35]. The exemplified 13.26-MHz WPT systems can achieve an overall system efficiency of 70%.

In practical applications, however, the variation of practical load resistances inevitably affects the maximum efficiency tracking scheme. Accordingly, an ON–OFF keying-based scheme was proposed to achieve the high efficiency within a wide-range load power [36], which has no requirement on an impedance-matching dc–dc power converter and thus reduce the switching loss. Additionally, by taking into account the variation of the loosely coupling effect, an integrated dynamic coupling-coefficient estimation scheme was proposed for the maximum efficiency tracking [37].

Apart from controlling the output voltage to adjust the equivalent load impedance, there are other attempts for the maximum efficiency tracking. For example, a multicycle Q-modulation can modulate the Q of the receiving coil and dynamically optimize the load impedance [38], which aims to ensure the maximum power transfer efficiency. Without requirement on a power or current sensor, a low-cost maximum efficiency tracking scheme was implemented to fulfill the load transformation by controlling a dc–dc converter [39]. In [40], a pulse-density modulation scheme was proposed by using the delta-sigma modulator and a dual-side soft switching technique, which can avoid disadvantages of the complexity, power loss, hard switching, low average efficiency, and dc voltage ripples.

B. Transmitted Power

The transmitted power capability is one of the most important performance indexes for WPT systems [41]–[43]. Due to working in a relatively high-frequency range, the power level is limited by the switching component, the topology of power-electronic inverters, and the associated control scheme.

Regarding to the switching component, an enhanced gallium nitride (eGaN) device was utilized to improve the output power capability in the MHz frequency band [44]. For the circuit topology, an LCL load resonant inverter was investigated for maximum power transfer [45], which is operated in the discontinuous current mode and controlled by a variable frequency scheme. The presented work successfully predicted the inverter operating point and ensured the optimal value of the series inductance. In [46], a multiphase parallel inverter was proposed to improve the output power capability for WPT systems. In [47], a 6-kW parallel IPT power supply topology was proposed in a cost effective manner, which can minimize uneven power sharing due to component tolerance without additional reactive components for parallelization. Regarding to the control scheme, an offline-tuning scheme was proposed to ensure the WPT system to output the maximum power instead of the online frequency regulation [48]. Accordingly, the constant operating frequency can effectively avoid the violation caused by the variation of operating frequency. The key to maximum power transfer is to ensure the impedance matching. In [49], a hybrid impedance-adjusting scheme was developed by combining the continuous conduction mode (CCM) and the discontinuous conduction mode (DCM), which can effectively extend the adjusting range and thus ensure the full utilization of the power capacitor for WPT systems.

C. Transmission Distance

By comparing with the photovoltaic, acoustic, microwave, and laser energy transmissions, the IPT has the salient advantage of high power. For long-distance transmission applications, however, the IPT system has to deal with inevitable key technical issue, namely the extremely loosely coupled effect. According to the measurement results in [50], the coupling coefficient κ is mostly much less than 0.01 with respect to the transmission distance from 2 to 12 m. As shown in Fig. 7, a dipole-coil-based

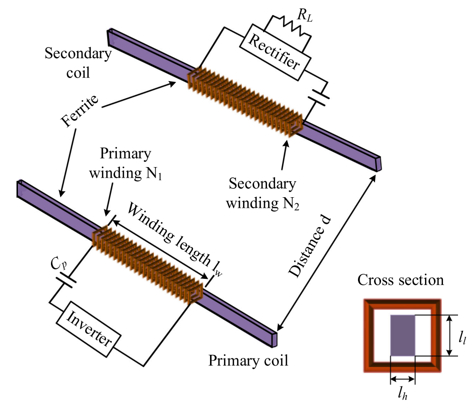

Fig. 7. Optimal dipole-shaped coils for long-distance IPT systems.

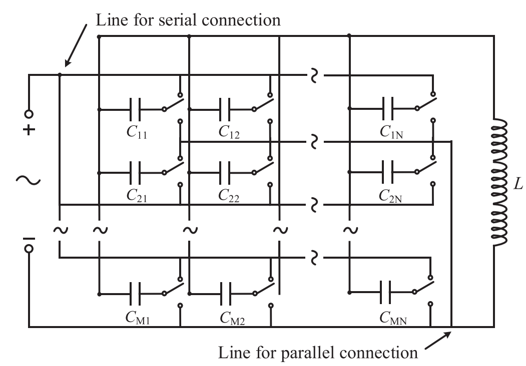

Fig. 8. Capacitor matrix for impedance matching.

IPT system was proposed for a long-distance energy transmission in [50] and [51], which adopts an optimized stepped core structure for evenly distributed magnetic field density. The experimental prototype can deliver 10.3 W power up to 7 m away at the frequency of 20 kHz.

In addition, due to the impact on the resonant frequency, the variation of the transmission distance is another important technical concern for IPT systems. In previous studies, consequently, there are a number of attempts for the impedance matching to ensure the magnetic resonant state even if a varying distance between the transmitting and receiving coils. As shown in Fig. 8, a capacitor matrix was proposed in [52], which can offer expected compensation capacitances by using limited capacitors to deal with the frequency mismatch caused by the varying transmission distance. In [53], a multiloops topology was utilized to reduce the variation of the input impedance.

D. Displacement Flexibility

As shown in Fig. 9, the WPT system is sensitive to the relative position between the transmitting and receiving coils, which means that the transmission performance is deteriorated with respect to an angular or lateral misalignment. The output power P_{out} of IPT systems can be given by [54], [55]

$$P_{\text{out}} \approx \eta P_{\text{in}} = \frac{\eta U_1^2 \,\text{Re}(Z_r)}{|Z_r|} \tag{11}$$

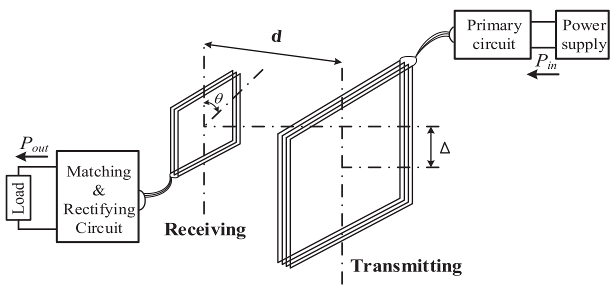

Fig. 9. Misalignment of WPT systems.

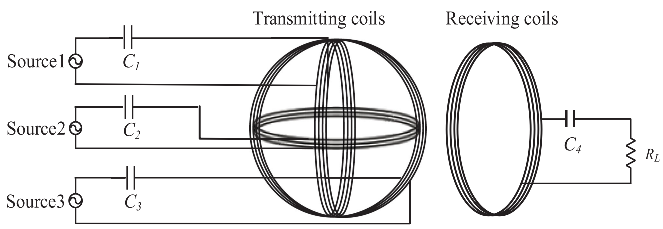

Fig. 10. Three-orthogonal-coil topology for omnidirectional WPT systems [65].

where P_{in} is the output power, η is the transmission efficiency, and Z_r is the reflected impedance from the secondary to the primary circuits. Accordingly, there are two ways to improve the misalignment tolerance, such as 1) optimizing the coil to alleviate the decay of the coupling effect [56] and 2) compensating the capacitance for the reflected impedance [54].

1) Coil Topology: The design of the asymmetrical loosely coupled transformer was proposed to reduce the deterioration of the misalignment for WPT systems by analyzing the impact of the coupling coefficient on the compensation network [58]. In [59] and [60], a three-dimensional (3-D) topology was implemented by adopting two orthogonal coils arranged in a spatial space aiming to reduce the sensitivity to the angular and the lateral misalignments of WPT systems.

2) Compensation Network: In [57], the current-controlled inductor and the variable switching frequency scheme were both adopted to ensure the optimal switching conditions for Class-E inverter of the primary side. The proposed power-electronic-based tuning scheme can effectively compensate the impact of the misalignment on the transmission performance. By comprehensively analyzing four basic compensation topologies as aforementioned in Section II, a series–parallel–series topology was proposed for both the primary and secondary sides in [61], aiming to ensure a high misalignment tolerance for WPT systems.

E. Omnidirectional Charging

The key of multiobjectives WPT system is to ensure the energy supply at an arbitrary spatial position. Accordingly, the omnidirectional WPT system is moving toward the center of the stage, which has been reported in previous studies [62]–[64]. For smart home applications, while a compact transmitter with the ability of middle and long-range transmission is suitable for indoor utilizations, as shown in Fig. 10, a transmitter with orthogonally assembled coils has been increasingly accepted by researchers since it can offer an enhanced flexible charging way for household appliances. Based on such an orthogonal topology, the current phase and amplitude modulation was proposed to spatially produce the electromagnetic field to cordlessly energize electric-driven devices [65]. In [66] and [67], the transmitter consisting of two vertical coils fed by current sources with adjusted amplitudes, which aims to generate a rotating electromagnetic field. In addition, the impact of the current phase was also studied for such a coil topology in [68], where a feeding phase difference of 90° was adopted to verify the capability of power transfer to a mobile receiver around the transmitter in a two-dimensional (2-D) space. In [69], a novel cubic transmitter was designed and fabricated to fulfill an omnidirectional WPT system by adopting one single power source. The presented work can simplify the control method while its capability of 3-D power transfer remains to be verified.

With the gradual in-depth research on omnidirectional WPT systems, its technical requirement is gradually clear up, namely the induced electromagnetic field can be not only distributed in a 3-D space effectively but also concentrated to the loads directionally. Then, the current amplitude control was proposed for a 3-D WPT system with a three-orthogonal-coils transmitter and a single load [65]. In order to further reveal its working mechanism, the corresponding mathematical model was built by extending from the 2-D to the 3-D coordinate [70]. Besides, the simulated and experimental verifications were also carried out to verify the electromagnetic field distribution and power control [71]. Such a coil topology is becoming one of the optimal technical solutions for the omnidirectional WPT systems.

F. Security

Along with the increasing studies on multiobjectives WPT systems, the security of the transmitted energy also attracts attentions from researchers. Especially for multiple energy receptors existing in an identical frequency electromagnetic field, the wireless charger needs encrypt the transmitted energy, which aims to ensure authorized receptors to acquire the expected power and meanwhile prevent unauthorized receptors from stealing the energy illegally. In 2015, the energy encryption scheme was first proposed and implemented for WPT systems in [72] and [73], where the characteristic of frequency sensitivity was positively utilized to encrypt the transmission channel. Specifically, the power supply purposely adjusts the transmission frequency according to the predefined regulation which is confidential and unpredictable for all potential energy receptors. Meanwhile, the capacitor array is adopted to adjust the impedance to match with the selected frequency value. Then, the transmitted energy can be packed with various frequencies and delivered by the specified time slot. Fig. 11 depicts the distribution of the electromagnetic field for the authorized and the unauthorized receptors. It illustrates that the magnetic flux density of the authorized receptor can achieve around 0.4 mT while it drops to an extremely low level for the unauthorized. Thus, the proposed energy encryption can effectively

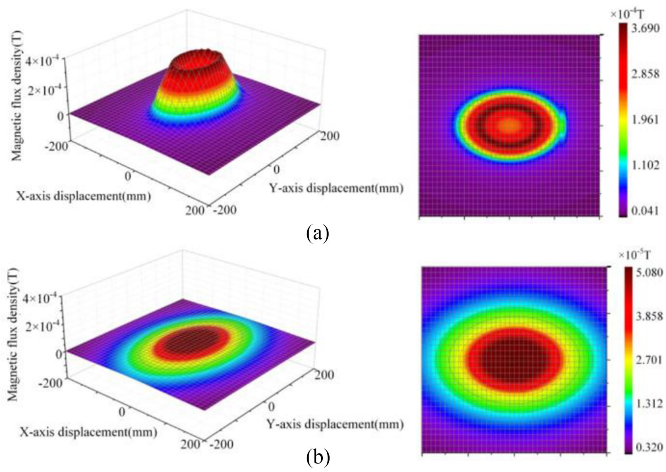

Fig. 11. Electromagnetic filed distribution. (a) Authorized receptor. (b) Unauthorized receptor.

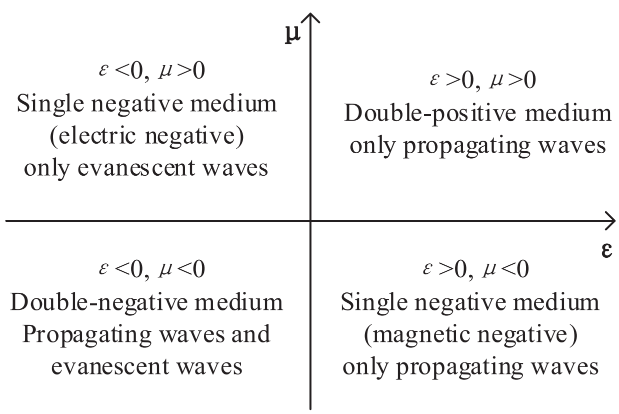

Fig. 12. Classification of materials with respect to ε and μ.

improve the security performance for multiobjectives WPT systems.

IV. Metamaterials

According to the electromagnetic parameters, Fig. 12 shows the classification of materials, where the first quadrant represents a classic type of regular dielectrics possessing the positive permeability μ and the positive permittivity ε. The materials in the second, third, and fourth quadrants have either negative ε or negative μ, or the both. As an artificial material in the third quadrant, the metamaterial has the negative permeability and the negative permittivity [74], which is commonly called as the left-handed material [75], [76]. By means of the double-negative characteristic, the metamaterial possesses abilities of amplifying the evanescent wave and concentrating the electromagnetic energy. Accordingly, the metamaterials exhibit great potentials to improve the energy transmission performance of WPT systems, especially for concentrating the distribution of the magnetic field and enhancing the magnetic flux density. There are increasing studies which have focused on the combination of metamaterials and WPT technologies.

The energy efficiency is the most important concern of WPT systems. The negative permeability can collect the leaking energy of the induced electromagnetic field and enhance the mutual inductive coupling effect, thus effectively increasing the energy efficiency. Fig. 13 summarizes previous studies on the optimization of the metamaterial slabs for WPT systems, such as one-dimensional (1-D) (planar), 2-D, and 3-D multiple-resonators topologies, as well as the relative position of metamaterial slabs against the transmitting and the receiving coils.

In [77], a hybrid metamaterial slab was proposed by combining two kinds of structures of metamaterial cells with the negative and the zero permeability for WPT systems. Along the transmission path between the transmitting and receiving coils, the proposed hybrid metamaterial slab can ensure that the inside magnetic field propagates straightly through the center due to the zero permeability while the outside magnetic field can be concentrated into the receiving coil through the edge of the proposed hybrid metamaterial slab due to the negative permeability. Accordingly, it can effectively increase the energy efficiency of the WPT system from 8.7% to 47% with the transmission distance of 20 cm and the operating frequency of 6.78 MHz. In [78], a double-side square spiral was developed as the unit cell of the metamaterial slab to optimize the performance. In [79], an experimental prototype was set up to carry out a comparative analysis for various metamaterial topologies, where a 40-W bulb can be wirelessly lighted with the distance of 50 cm and the frequency of 27.12 MHz. Based on the brightness of the bulb, it verifies the effectiveness of the metamaterial to improve the energy efficiency of WPT systems. Besides, there are increasing studies on the 3-D metamaterial to further improve the transmission efficiency of WPT systems. In [80] and [81], a 6×6-array metamaterial slab was proposed to wirelessly light up a 15-W bulb, where the unit cells are periodically assembled on a 5-mm thick acrylic slab forming a 6×6 array. The experimental prototype consists of a source coil, a load coil connected with a bulb, the metamaterial slab placed between the transmitter and receiver, and a transmitting coil and a receiving coil resonating at 6.78 MHz. The experimental results show that the 3-D metamaterial slab can increase the transmission efficiency by 24%. In [82], a 3-D metamaterial structure was proposed for midrange WPT systems, which consists of a $4 \times 5 \times 1$-array of three-turn spiral resonators with the negative permeability at the frequency of 6.5 MHz. The corresponding experimental results show that the output power can be increased by 33% and 7.3% at distances of 1.0 and 1.5 m, respectively. Thus, it can verify the effectiveness of 3-D metamaterial topology to increase the energy efficiency and the transmission distance for WPT systems. Apart from the studies on the topology of metamaterial slabs, its locating position is also attracted attentions. Additionally, the exemplified prototype adopts two 3-D metamaterial slabs locating adjacent to the source and receiving coils, respectively, including in front of coils [83] and back of coils [84]. This is the main difference from the previous studies, which normally adopted one single slab locating in the middle of the transmission path. The measured results show that the energy efficiency increases to approximately 80% at a distance of 1.5 m. More

Metamaterial-based WPT											
Topology						Position					
Topic	Ref.	P [W]	η [%]	f [MHz]	d [cm]	Topic	Ref.	P [W]	η [%]	f [MHz]	d [cm]
1-D slab	[77]	-	47	6.78	20	Middle of path	[78]	80	34	27.12	50
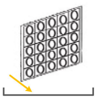	[79]	40	47	27	50	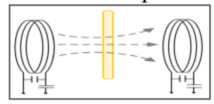	[80]-[81]	15	~40	6.78	60
	[80]-[81]	15	~40	6.78	60		[82]	-	33/7.3	6.5	100/150
	[86]	40	85_{peak}	25	5		[86]	40	85_{peak}	25	5
2-D slab	[78]	80	34	27.12	50	Front of coils	[80]	15	36.7	6.78	60
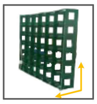	[79]	40	47	27	50	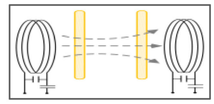	[81]	15	40	6.78	60
	[81]	15	40	6.78	60		[83]	-	80	23.2	150
	-	-	-	-	-		[85]	-	57.9	6.6	100
3-D slab	[81]	15	40	6.78	60	Back of coils	[84]	80	34	27.12	50
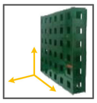	[82]	-	33/7.3	6.5	100/150	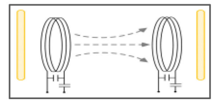	-	-	-	-	-
	[83]	-	80	23.2	150		-	-	-	-	-
	-	-	-	-	-		-	-	-	-	-

Fig. 13. Classification of previous studies on metamaterial-based WPT technologies.

importantly, the practicability of metamaterial-based WPT technique is improved significantly.

Besides, the metamaterial slab can be also used as an effective means to compensate the deteriorated transmission performance caused by the misalignment. In [85], the H-field distribution of the exemplified metamaterial-based WPT systems illustrates that the coupling effect can be enhanced when existing a lateral or angular misalignment between the transmitting and receiving coils. In particular, the metamaterial slab has salient advantage of compensating the energy efficiency of WPT systems with respect to an angular misalignment. In [86] and [87], an array of metamaterial resonators was designed for dynamic wireless charging systems, which are embedded into the transmitting coil array beneath the road or the power track. The results show that the efficiency can achieve to around 75%. Thus, the metamaterial exhibits great potentials for enhancing the energy efficiency of static and dynamic charging systems, especially for the lateral and angular misalignment.

V. Applications

WPT techniques offer abilities of harnessing the energy over the air. Without the limitation of the conventional wire, the electric-driven devices possess the unprecedented flexibility of energy accessing. The dynamic contactless charging technique is coming to our daily life. In this section, this paper will have a survey on typical applications for WPT technologies, including EVs, biomedical implants, and portable electronics.

A. Electric Vehicles (EVs)

For wirelessly energizing EVs, there are two distinct but effective implementation mechanisms, that is, the resonant CCPT [88]–[91] for dynamic wireless charging and the resonant IPT [92] for both static wireless charging and dynamic wireless charging. Regarding to the static EV wireless charging, it means that the only thing which the driver needs to do is just parking the car at the specific position. Then, the battery can be charged via coupled magnetic field between the transmitting and the receiving coils. For the dynamic wireless charging, the vehicle can continuously acquire the energy when driving on a road. By means of this novel energy acquisition scheme, the battery capacity of EVs can be reduced to more than 20% by comparing to the traditional plug-in EVs [92], which shows significant meanings for the further development and the wide application of EVs in our daily life. Accordingly, this section will overview the WPT technique for EVs in terms of the coupling mechanism, the resonant compensation, and the control strategy. Finally, a future research topic will be also discussed in this paper.

1) Design and Optimization of Coupling Mechanism: The key technical challenge is to increase the coupling coefficient κ while reducing the magnetic flux leakage. Besides, the misalignment tolerance is another technical concern for EV wireless charging systems. In previous studies, a number of attempts have been made for aforementioned issues. From the perspective of materials, the high permeability material such as ferrites and the aluminum plate are utilized as the magnetic flux guide and the shield [93], respectively, which can effectively improve the effective magnetic field density and reduce the flux leakage. Besides, the Litz wire consisting multiple strands is commonly used to wrap the transmitting coils in both sides [94], which aims to avoid the skin effect and the proximity effect.

Additionally, regarding to the similar dimension, the difference of the coil geometry and configuration results in a significant difference of the magnetic coupling effect. Hence, the optimal design is necessary for the coil of EV wireless charging systems. For example, the circular-shaped and square-shaped transmitting coils are mostly used for EV static wireless charging systems [95]. In addition, a new coil topology was proposed by placing two coils shaped like "D" back to back [96], which is called as the double D (DD) structure. By comparing with a

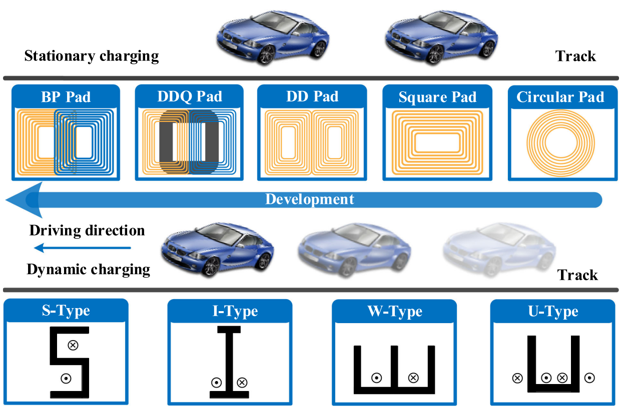

Fig. 14. Coils and ferrites topologies for EV charging.

conventional single circular-shaped or square-shaped pad, the DD charging pad can effectively enhance the lateral misalignment tolerance, thus increasing the effective charging area for EV drivers. In [97], an asymmetric coil structure was investigated for EV static charging, which can also offer an enhanced misalignment tolerance.

For EV charging systems, the coil design should take into account especially for the area between two adjacent transmitting coils, the magnetic flux density drops to an extremely low level. It means that there are many energy valleys along the driving road. In other word, EVs cannot constantly obtain the energy. Accordingly, a homogenous WPT structure was proposed for transmitting coils beneath the road by using the alternating winding design to gaplessly assemble transmitting coils [98], which can effectively fill up the energy valley and fulfill a continuous charging mechanism for driving EVs. Apart from the work on the primary side, a DD-quadrature (DDQ) coil was designed for the receiving coil on the EV side [99]. The additional Q coil increases the capability of acquiring energy around the gap between adjacent coils, thus significantly improve the charging performance. By increasing the size of D coils and overlapping them, the new bipolar pad can reduce the copper by 25.17% while ensure the performance as a DDQ coil [100], [101]. For EV dynamic charging, previous studies have reported various ferrites to increase the coupling effect and ensure the charging performance [102], [103], such as E-type, U-type, and W-type. In [104], a narrow-width track design with an I-type ferrite was proposed to further reduce the volume of track rail, improve the convenience of laying transmitting coils, and reduce costs. In [105], an S-type ferrite was designed to further enhance the misalignment tolerance for EV wireless charging systems. Fig. 14 summarizes typical coil topologies for EV static and dynamic charging systems.

2) Compensation Topologies and Control Strategies: Apart from four typical compensation networks [106], the *LCL* topology was investigated for EV dynamic charging systems [107]–[109]. It can be used as a current source at the resonant frequency, thus avoiding short circuit in the pickup side and the overcurrent in the primary side. In other word, the *LCL* compensation network can realize the constant current and the unity-power-factor. In [110]–[112], the *LCC* compensation topology was proposed to realize a robust reaction to the variation of coupling effect, which is one of the most common technical issue for EV dynamic charging systems. The proposed double-sided *LCC* compensation network can ensure that the resonant frequency is independent of coupling coefficient and load conditions as well as realizing the zero voltage switching condition for the power converter.

In addition, a number of control schemes have been reported for EV dynamic charging systems in previous studies, which can be classified into three directions, that is, the primary side control [104], [113], the pick-up side control [93], and the dual-side control [114], [115]. The primary side and dual-side control schemes are commonly suitable for monocoupling charging system, while the pick-up side control is utilized in the multi-coupling charging systems.

3) Wireless Vehicle-to-Grid (V2G): The V2G takes EVs as movable energy buffers, which can effectively balance the power supply and the load. As the key power device, the bidirectional EV charger has been attracted increasing attentions from researcher around the world. Along with the development of EV wireless charging, the bidirectional contactless energy exchange will be increasingly important. Actually, there have been several attempts for wireless interaction between the power grid and EVs [116].

B. Biomedical Implants

In recent years, the implantable biomedical devices have been one of the most important ways to assist the treatment for dysfunctional organs therapeutically. The corresponding energization has attracted increasing attentions from researchers around the world, accordingly. Based on the two-port network, the analysis of near-field power transfer and associated optimization strategies were overviewed for biomedical implants in [117]. As a summarization, the major technical challenges are listed as follows.

1) Energy Efficiency: In [118], a modified Helmholtz coil was designed to produce a uniform magnetic field for the improvement of the power stability for powering robotic capsules. In addition, a mixed resonance scheme was also employed to improve the transmission efficiency. In [119], a novel circuit model of the subnominal class-E amplifier was proposed for capsule endoscopes. By analyzing the impact of the amplifier parameters, an optimal subnominal condition was derived for the amplifier design to ensure the high efficiency and safe voltage stress. For millimeter-sized biomedical implants, the energy efficiency can be improved by simply increasing the frequency, while the maximum allowable power is inevitably deteriorated, accordingly. In [120], a new figure-of-merit (FOM) was proposed for the optimal geometry of the transmitting and receiving coils under safety constrains, which can strike a balance between the energy efficiency and the maximum transmitted power.

2) Varying Load: In [121], a triple-loop WPT system was proposed by adopting the closed-loop power control, the adaptive transmitting resonance compensation, and the automatic receiving resonance tuning, which can ensure the maximum the efficiency with respect to varying surrounding environment for implants. In [122], this paper proposed a frequency control scheme for the primary converter to ensure the transmitted power even if the variations of the load, coupling effect, and parameters, which show significant meanings for biomedical implants. By using the printed circuit board (PCB) pattern coil and the complementary metal oxide semiconductor (CMOS) switch, the parallel resonance topology and associated frequency-tracking scheme were proposed for biomedical implants, which aim to improve the efficiency and maintain a constant output voltage under varying against the variations of the coupling at the load [123].

3) Misalignment: By taking into account the specific absorption rate, an optimal design scheme was proposed by using a high-Q receiving coil and a large external transmitting coil, which can effectively energize the millimeter-sized free-floating implants in a large 3-D space in the neural tissue in [124]. In order to ensure a motion-free capsule endoscopy inspection, a two-hop WPT system was designed in [125], where the energy is wirelessly transmitted from the transmitting coils beneath the floor to the coil relay embedded in patient's jacket via the strong coupling effect, and then to the capsule via the loose coupling. Additionally, a switch-mode rectifier and a power combination circuit were also developed to improve the energy efficiency for robot capsules.

4) Safety Concerns: Besides, a coil segmentation technique was proposed to ensure the transmitter voltage at a safe level ($\sim 10V_{\rm rms}$) for midrange WPT systems in [126], which can be used to wirelessly energize a dc pump for artificial hearts or left ventricular assist devices.

C. Portable Electronics

Due to disadvantages of tangled and inconvenient power cords, the WPT shows promising future for portable electronics. Nowadays, there are two major technical alliances about the wireless charging for portable electronic devices, including the Wireless Power Consortium with the Qi standard released in 2008 and the Air Fuel Alliance founded in 2015 by merging the Alliance for Wireless Power and the Power Matters Alliance.

These two standards are both based on the inductive charging technology and now attempting to integrate both the inductive and the resonant technology into single product. The main difference between Qi and Air Fuel Alliance is the transmission frequencies and communication protocols that support the in-band communication, namely the power and data. Specifically, the Qi-compliant wireless charging devices transmissions share the same frequency band, while the Air Fuel Alliance adopts the out-of-band communication, namely 6.78 MHz Industrial Scientific Medical (ISM) frequency band for the power transmission and 2.4 GHz ISM band for the communication. Furthermore, some products provided by the Air Fuel Alliance are able to charge multiple devices with respect to different power requirements by using one single power source in the primary side.

VI. Conclusion

In this paper, the WPT techniques were overviewed with emphasis on fundamentals, technical challenges, metamaterials, and typical applications. Regarding to the fundamentals, this paper first introduced the working mechanism of IPT systems, compared four typical capacitive compensation networks, and then elaborated the magnetic resonant coupling effect as well as the CCPT mechanism. In Section II, this paper gave the answers to two technical questions, namely 1) why the two-coils IPT system is commonly used for short-range (shorter than the coil diameter) transmission and 2) why the four-coils IPT system can extend the transmission distance to the midrange applications. Then, the key technical issues of WPT systems were summarized in terms of the efficiency, power, distance, misalignment, omnidirectional charging, and energy security. In addition, this paper also offered a survey on the studies of metamaterial-based WPT systems. Finally, the typical applications was also discussed, including EVs, biomedical implants, and the portable electronics. By overviewing the development and the current state over past six years, this paper is expected to offer readers a big image of WPT techniques based on the inductive coupling effect of nonradiative electromagnetic field. Moreover, Table II elaborated the critical technical details for various aspects.

In addition the discussion about the future development is also given as follows.

1) *Transmission distance*—The transmission distance will be the most important concern for both researchers and end-users. A real WPT system should harness the energy over a long distance rather than the wireless-but-contact charging style. However, a long distance means extremely loosely coupling effect for electromagnetic WPT systems. How to break through this technical bottleneck will be the focus of attention in near future.
2) *Energy security*—As similarity with the development of wireless communication, the security of energy will be another key technical challenge for the further development of WPT systems. Regarding to the IPT system, the energy was transmitted via the open electromagnetic field. In other word, it is possible for all involved receptors to access the energy. Then, how to protect the wirelessly-transmitted energy will be an inevitable research topic.
3) *Bidirectional exchange*—As one of typical applications, EVs will be further developed and wide popularized, even completely replacing the conventional internal combustion engine vehicles. In such a case, the energy acquisition will be increasingly important for EVs. As aforementioned, in addition, the V2G technique can make EVs as movable energy buffers, which can effectively balance the power supply and the load. Thus, the bidirectional EV wireless charging will be next hot research topic after the roadway-powering mechanism.

TABLE II
CONTENT

Challenges		Methods
Efficiency	**Control** (MEPT, CV/CI)	[29], [32]-[34], [38], [40] Maximum efficiency tracking control for closed-loop systems: a. Phase-shift and amplitude control b. Maximum efficiency point tracking control c. Employing series resonant tank d. Pulse density modulation e. A multicycle Q-modulation f. An active-rectifier-based maximum efficiency tracking method using an auxiliary measurement coil. [36] On-off keying-based scheme: any s-s resonant WPT system operating at constant output voltage. [37] An integrated dynamic coupling-coefficient estimation scheme.
Efficiency	**Coupling** (Coil, Mechanism)	[14] A ceramic based dielectric between the parallel plates. [18] A six-plate capacitive coupler: power density of 1.95 kW/m2 and dc–dc efficiency of 91.6% with an air-gap of 150 mm. [21] Combined inductive and capacitive mechanism with LC-compensated topology: 2.84-kW output power with 94.5% efficiency with a switching frequency of 1-MHz. [25] A non-unity Track-Width-Ratio geometrical: improve hollow planar spiral winding. [26] An intermediate coil: 6.6-kW of output power with an overall 95.57% efficiency with a switching frequency of 100kHz at an air gap of 200 mm. [27] U-coil system: the dimension of transmitting and secondary coils in U-coil system shrinks at least 66% comparing with that of two-coil system with the same power transfer efficiency principle. [28] Series-shunt mixed-resonant coupling topology: efficiency of 85% at a distance of 10 cm.
Efficiency	**Circuit** (Compensation, Converter)	[16] Suboptimal Class-E^2 converter: develop an auto-frequency tuning mechanism based on a PI approach. [17] A double-sided LC-compensation: dc–dc efficiency higher than 70% across an air-gap of 180 mm with a switching frequency of 1.5-MHz. [24] Semi-resonant Class-E driver: a dc-to-load efficiency above 77% with a switching frequency of 6 MHz [31] Switched-mode converter: emulate the optimal load value in the receiver module. [35] Cascaded Buck-Boost converter: provide the optimal impedance matching in WPT system for various loads including resistive load, ultra-capacitors, and batteries.
Power	**Control** (Impedance matching, MPPT)	[45] A LCL load resonant inverter: predict the inverter operating point and enable the optimum value of the series inductance to be found. [48] An optimal coupling using frequency splitting: adjust the capacitance of the resonator. [49] An hybrid impedance matching range extension method based on combined continuous conduction mode (CCM) and discontinuous conduction mode (DCM).
Power	**Circuit** (Topology)	[44] An enhanced gallium switching nitride (eGaN) device with a single-ended class ϕ_2 inverter topology. [46] A multiphase parallel inverter: 20-kW output power with 95.6% efficiency with an air-gap of 200 mm. [47] A parallel topology for LCL-T-based IPT power supplies: minimize uneven power.
Distance	**Coupling** (Coil)	[50] A dipole-coil-based extremely loosely coupled IPT system (IPTS) for wireless sensors over a wide range: 10.3-W output power with a switching frequency of 20-kHz at an air-gap of 7m. [51] Magnetic dipole type coils with cores: an optimized stepped core structure.
Distance	**Circuit** (Topology, Compensation)	[52] A novel capacitor matrix for an adaptive impedance-matching network: efficiency of 88% with 1-W output power with a switching frequency of 13.56-MHz at an air-gap of changes from 0 to 1.2 m. [53] Multi-loops topology: reduce the variation in the input impedance: efficiency of 92% at a distance of 10 cm. [109] A double-sided LCLC-compensation: 2.1-kW output power with 90.7% efficiency at an air-gap of 300 mm.
Misalignment	**Coupling** (Structure)	[56] Figure of merit (FOM): optimize six-DoF misalignment tolerance. [58] Asymmetrical LCT prototype: compared to the symmetrical LCT architecture, the proposed asymmetrical LCT prototype improves the coupling coefficient reduction from 68% to 28% when the gap varies from 6 to 20 mm and from 89% to 31% when the misalignment ranges from 0 to 50 mm. [60] Two orthogonal coils arranged in a spatial space.
Misalignment	**Circuit** (Topology)	[54] Optimize compensation capacitor: the tolerant lateral misalignment extended to 44.3% of the coil size with a 38.3% relative improvement. [59] A novel set of SCMR-based topology: 40% efficiency for the entire range of 360° of angular misalignment.
EMI		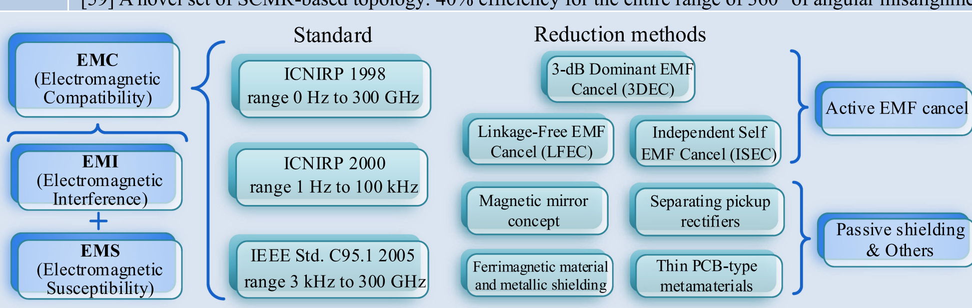
Security		[72] [73] Energy is encrypted by confidentially regulating the frequency of the power source.

REFERENCES

[1] C. T. Rim and C. Mi, *Wireless Power Transfer for Electric Vehicles and Mobile Devices*. Hoboken, NJ, USA: Wiley-IEEE Press, 2017.

[2] S. Y. R. Hui, W. Zhong, and C. K. Lee, "A critical review of recent progress in mid-range wireless power transfer," *IEEE Trans. Power Electron.*, vol. 29, no. 9, pp. 4500–4511, Sep. 2014.

[3] K. T. Chau, *Electric Vehicle Machines and Drives – Design, Analysis and Application*. Hoboken, NJ, USA: Wiley-IEEE Press, 2015.

[4] G. A. Covic and J. T. Boys, "Inductive power transfer," *Proc. IEEE*, vol. 101, no. 6, pp. 1276–1289, Jun. 2013.

[5] I. Mayordomo, T. Drager, P. Spies, J. Bernhard, and A. Pflaum, "An overview of technical challenges and advances of inductive wireless power transmission," *Proc. IEEE*, vol. 101, no. 6, pp. 1302–1311, Jun. 2013.

[6] C. Qiu, "Design, analysis and application of dynamic wireless power transfer," *Ph.D. dissertation*, Univ. Hong Kong, Hong Kong, 2016.

[7] Z. Zhang, "Energy cryptography for wireless charging of electric vehicles," in *Energy Systems for Electric and Hybrid Vehicles*. Herts, U.K.: Inst. Eng. Technol., 2016, ch. 11, pp. 319–417.

[8] Y. H. Sohn, B. H. Choi, E. S. Lee, G. C. Lim, G. H. Cho, and C. T. Rim, "General unified analyses of two-capacitor inductive power transfer systems: Equivalence of current-source SS and SP compensations," *IEEE Trans. Power Electron.*, vol. 30, no. 11, pp. 6030–6045, Nov. 2015.

[9] J. Zhang, X. Yuan, C. Wang, and Y. He, "Comparative analysis of two-coil and three-coil structures for wireless power transfer," *IEEE Trans. Power Electron.*, vol. 32, no. 1, pp. 341–352, Nov. 2017.

[10] A. Kurs, A. Karalis, R. Moffatt, J. D. Joannopoulos, P. Fisher, and M. Soljačić, "Wireless power transfer via strongly coupled magnetic resonances," *Science*, vol. 317, no. 5834, pp. 84–86, 2007.

[11] S. Cheon, Y.-H. Kim, S.-Y. Kang, M. L. Lee, J.-M. Lee, and T. Zyung, "Circuit-model-based analysis of a wireless energy-transfer system via coupled magnetic resonances," *IEEE Trans. Ind. Electron.*, vol. 58, no. 7, pp. 2906–2914, Jul. 2011.

[12] C. Liu, A. P. Hu, and N. C. Nair, "Modelling and analysis of a capacitively coupled contactless power transfer system," *IET Power Electron.*, vol. 4, no. 7, pp. 808–815, 2011.

[13] J. Dai and D. C. Ludois, "Single active switch power electronics for kilowatt scale capacitive power transfer," *IEEE J. Emerg. Sel. Topics Power Electron.*, vol. 3, no. 1, pp. 315–323, Mar. 2015.

[14] S. K. Mishra, R. Adda, S. Sekhar, A. Joshi, and A. K. Rathore, "Power transfer using portable surfaces in capacitively coupled power transfer technology," *IET Power Electron.*, vol. 9, no. 5, pp. 997–1008, 2016.

[15] C. Liu, A. P. Hu, G. A. Covic, and N. C. Nair, "Comparative study of CCPT systems with two different inductor tuning positions," *IEEE Trans. Power Electron.*, vol. 27, no. 1, pp. 294–306, Jan. 2012.

[16] K. Lu, S. K. Nguang, S. Ji, and L. Wei, "Design of auto frequency tuning capacitive power transfer system based on class-E^2 dc/dc converter," *IET Power Electron.*, vol. 10, no. 12, pp. 1588–1595, 2017.

[17] F. Lu, H. Zhang, H. Hofmann, and C. Mi, "A double-sided LC-compensation circuit for loosely coupled capacitive power transfer," *IEEE Trans. Power Electron.*, vol. 33, no. 2, pp. 1633–1643, Feb. 2018.

[18] H. Zhang, F. Lu, H. Hofmann, W. Liu, and C. Mi, "Six-plate capacitive coupler to reduce electric field emission in large air-gap capacitive power transfer," *IEEE Trans. Power Electron.*, vol. 33, no. 1, pp. 665–675, Jan. 2018.

[19] Y. G. Su, W. Zhou, A. P. Hu, C. S. Tang, S. Y. Xie, and Y. Sun, "Full-duplex communication on the shared channel of a capacitively coupled power transfer system," *IEEE Trans. Power Electron.*, vol. 32, no. 4, pp. 3229–3239, Apr. 2017.

[20] J. Dai and D. C. Ludois, "A survey of wireless power transfer and a critical comparison of inductive and capacitive coupling for small gap applications," *IEEE Trans. Power Electron.*, vol. 30, no. 11, pp. 6017–6029, Nov. 2015.

[21] F. Lu, H. Zhang, H. Hofmann, and C. Mi, "An inductive and capacitive combined wireless power transfer system with LC-compensated topology," *IEEE Trans. Power Electron.*, vol. 31, no. 12, pp. 8471–8482, Dec. 2016.

[22] D. C. Ludois, J. K. Reed, and K. Hanson, "Capacitive power transfer for rotor field current in synchronous machines," *IEEE Trans. Power Electron.*, vol. 27, no. 11, pp. 4638–4645, Dec. 2012.

[23] C. Liu, A. P. Hu, B. Wang, and N. C. Nair, "A capacitively coupled contactless matrix charging platform with soft switched transformer control," *IEEE Trans. Ind. Electron.*, vol. 60, no. 1, pp. 249–260, Jan. 2013.

[24] M. Pinuela, D. C. Yates, S. Lucyszyn, and P. D. Mitcheson, "Maximizing DC-to-load efficiency for inductive power transfer," *IEEE Trans. Power Electron.*, vol. 28, no. 5, pp. 2437–2447, May 2013.

[25] S. R. Cove, M. Ordonez, N. Shafiei, and J. Zhu, "Improving wireless power transfer efficiency using hollow windings with track-width-ratio," *IEEE Trans. Power Electron.*, vol. 31, no. 9, pp. 6524–6533, Sep. 2016.

[26] S. Moon, B.-C. Kim, S.-Y. Cho, C.-H. Ahn, and G.-W. Moon, "Analysis and design of a wireless power transfer system with an intermediate coil for high efficiency," *IEEE Trans. Power Electron.*, vol. 61, no. 11, pp. 5861–5870, Nov. 2014.

[27] Z. H. Ye, Y. Sun, X. Dai, C. S. Tang, Z. H. Wang, and Y. G. Su, "Energy efficiency analysis of U-coil wireless power transfer system," *IEEE Trans. Power Electron.*, vol. 31, no. 7, pp. 4809–4817, Jul. 2016.

[28] L. Chen, S. Liu, Y. C. Zhou, and T. J. Cui, "An optimizable circuit structure for high-efficiency wireless power transfer," *IEEE Trans. Ind. Electron.*, vol. 60, no. 1, pp. 339–349, Jan. 2013.

[29] R. K. Mai, Y. R. Liu, Y. Li, P. F. Yue, G. Z. Cao, and Z. Y. He, "An active-rectifier-based maximum efficiency tracking method using an additional measurement coil for wireless power transfer," *IEEE Trans. Power Electron.*, vol. 33, no. 1, pp. 716–728, Jan. 2018.

[30] W. Zhang, S.-C. Wong, C. K. Tse, and Q. Chen, "Analysis and comparison of secondary series- and parallel-compensated inductive power transfer systems operating for optimal efficiency and load-independent voltage-transfer ratio," *IEEE Trans. Power Electron.*, vol. 29, no. 6, pp. 2979–2990, Jun. 2014.

[31] W. X. Zhong and S. Y. R. Hui, "Maximum energy efficiency tracking for wireless power transfer systems," *IEEE Trans. Power Electron.*, vol. 30, no. 7, pp. 4025–4034, Jul. 2015.

[32] A. Berger, M. Agostinelli, S. Vesti, J. A. Oliver, J. A. Cobos, and M. Huemer, "A wireless charging system applying phase-shift and amplitude control to maximize efficiency and extractable power," *IEEE Trans. Power Electron.*, vol. 30, no. 11, pp. 6338–6348, Nov. 2015.

[33] H. C. Li, J. Li, K. P. Wang, W. J. Chen, and X. Yang, "A maximum efficiency point tracking control scheme for wireless power transfer systems using magnetic resonant coupling," *IEEE Trans. Power Electron.*, vol. 30, no. 7, pp. 3998–4008, Jul. 2015.

[34] T. D. Yeo, D. Kwon, S. T. Khang, and J. W. Yu, "Design of maximum efficiency tracking control scheme for closed-loop wireless power charging system employing series resonant tank," *IEEE Trans. Power Electron.*, vol. 32, no. 1, pp. 471–478, Jan. 2017.

[35] M. Fu, C. Ma, and X. Zhu, "A cascaded boost-buck converter for high-efficiency wireless power transfer systems," *IEEE Trans. Ind. Informat.*, vol. 10, no. 3, pp. 1972–1980, Aug. 2014.

[36] W. Zhong and S. Y. R. Hui, "Maximum energy efficiency operation of series-series resonant wireless power transfer systems using on-off keying modulation," *IEEE Trans. Power Electron.*, vol. 33, no. 4, pp. 3595–3603, Apr. 2018. doi: 10.1109/TPEL.2017.2709341.

[37] X. Dai, X. Li, Y. Li, and P. Hu, "Maximum efficiency tracking for wireless power transfer systems with dynamic coupling coefficient estimation," *IEEE Trans. Power Electron.*, vol. 33, no. 6, pp. 5005–5015, Jun. 2018. doi: 10.1109/TPEL.2017.2729083.

[38] B. Lee, P. Yeon, and M. Ghovanloo, "A multi-cycle Q-modulation for dynamic optimization of inductive links," *IEEE Trans. Ind. Electron.*, vol. 63, no. 8, pp. 5091–5100, Aug. 2016.

[39] X. Tang, J. Zeng, K. P. Pun, S. Mai, C. Zhang, and Z. Wang, "Low-cost maximum efficiency tracking method for wireless power transfer systems," *IEEE Trans. Power Electron.*, vol. 33, no. 6, pp. 5317–5329, Jun. 2018. doi: 10.1109/TPEL.2017.2726085.

[40] H. Li, J. Fang, S. Chen, K. Wang, and Y. Tang, "Pulse density modulation for maximum efficiency point tracking of wireless power transfer systems," *IEEE Trans. Power Electron.*, vol. 33, no. 6, pp. 5492–5501, Jun. 20182017. doi: 10.1109/TPEL.2017.2737883.

[41] M. P. Kazmierkowski and A. J. Moradewicz, "Unplugged but connected: Review of contactless energy transfer systems," *IEEE Ind. Electron. Mag.*, vol. 6, no. 4, pp. 47–55, Dec. 2012.

[42] C.-S. Wang, G. Covic, and O. H. Stielau, "Power transfer capability and bifurcation phenomena of loosely coupled inductive power transfer systems," *IEEE Trans. Ind. Electron.*, vol. 51, no. 1, pp. 148–157, Feb. 2004.

[43] A. P. Sample, D. T. Meyer, and J. R. Smith, "Analysis, experimental results, and range adaptation of magnetically coupled resonators for wireless power transfer," *IEEE Trans. Ind. Electron.*, vol. 58, no. 2, pp. 544–554, Feb. 2011.

[44] J. Choi, D. Tsukiyama, Y. Tsuruda, and J. M. R. Davila, "High-frequency, high-power resonant inverter with eGaN FET for wireless power transfer," *IEEE Trans. Power Electron.*, vol. 33, no. 3, pp. 1890–1896, Mar. 2018.

[45] C. S. Wang, G. A. Covic, and O. H. Stielau, "Investigating an LCL load resonant inverter for inductive power transfer applications," *IEEE Trans. Power Electron.*, vol. 19, no. 4, pp. 995–1002, Jul. 2004.

[46] Q. J. Deng, J. T. Liu, D. Czarkowski, W. S. Hu, and H. Zhou, "An inductive power transfer system supplied by a multiphase parallel inverter," *IEEE Trans. Ind. Electron.*, vol. 64, no. 9, pp. 7039–7048, Sep. 2017.

[47] H. Hao, G. A. Covic, and J. T. Boys, "A parallel topology for inductive power transfer power supplies," *IEEE Trans. Power Electron.*, vol. 29, no. 3, pp. 1140–1151, Mar. 2014.

[48] D.-W. Seo, J.-H. Lee, and H.-S. Lee, "Optimal coupling to achieve maximum output power in a WPT system," *IEEE Trans. Ind. Electron.*, vol. 31, no. 6, pp. 3994–3998, Jun. 2016.

[49] X. Dai, X. Li, Y. Li, and P. Hu, "Impedance matching range extension method for maximum power transfer tracking in IPT system," *IEEE Trans. Power Electron.*, vol. 33, no. 5, pp. 4419–4428, May 2018. doi: 10.1109/TPEL.2017.2716968.

[50] B. H. Choi, V. X. Thai, E. S. Lee, J. H. Kim, and C. T. Rim, "Dipole-coil-based wide-range inductive power transfer systems for wireless sensors," *IEEE Trans. Ind. Electron.*, vol. 63, no. 5, pp. 3158–3167, May 2016.

[51] C. Park, S. Lee, G. H. Cho, and C. T. Rim, "Innovative 5-m-off-distance inductive power transfer systems with optimally shaped dipole coils," *IEEE Trans. Power Electron.*, vol. 30, no. 2, pp. 817–827, Feb. 2015.

[52] Y. Lim, H. Tang, S. Lim, and J. Park, "An adaptive impedance-matching network based on a novel capacitor matrix for wireless power transfer," *IEEE Trans. Power Electron.*, vol. 29, no. 8, pp. 4403–4413, Aug. 2014.

[53] J. Kim and J. Jeong, "Range-adaptive wireless power transfer using multiloop and tunable matching techniques," *IEEE Trans. Ind. Electron.*, vol. 62, no. 10, pp. 6233–6241, Oct. 2015.

[54] Q. Zhu, Y. Guo, L. Wang, C. Liao, and F. Li, "Improving the misalignment tolerance of wireless charging system by optimizing the compensate capacitor," *IEEE Trans. Ind. Electron.*, vol. 62, no. 8, pp. 4832–4836, Aug. 2015.

[55] V. Prasanth and P. Bauer, "Distributed IPT systems for dynamic powering: Misalignment analysis," *IEEE Trans. Ind. Electron.*, vol. 61, no. 11, pp. 6013–6021, Nov. 2014.

[56] J. P. K. Sampath, A. Alphones, and D. M. Vilathgamuwa, "Figure of merit for the optimization of wireless power transfer system against misalignment tolerance," *IEEE Trans. Power Electron.*, vol. 32, no. 6, pp. 4359–4369, Jun. 2017.

[57] S. Aldhaher, P. C. K. Luk, and J. F. Whidborne, "Electronic tuning of misaligned coils in wireless power transfer systems," *IEEE Trans. Power Electron.*, vol. 29, no. 11, pp. 5975–5982, Nov. 2014.

[58] C. Zheng, H. B. Ma, J. S. Lai, and L. H. Zhang, "Design considerations to reduce gap variation and misalignment effects for the inductive power transfer system," *IEEE Trans. Power Electron.*, vol. 30, no. 11, pp. 6108–6119, Nov. 2015.

[59] D. Liu, H. Hu, and S. V. Georgakopoulos, "Misalignment sensitivity of strongly coupled wireless power transfer systems," *IEEE Trans. Power Electron.*, vol. 32, no. 7, pp. 5509–5519, Jul. 2017.

[60] J. P. W. Chow, N. Chen, H. S. H. Chung, and L. L. H. Chan, "An investigation into the use of orthogonal winding in loosely coupled link for improving power transfer efficiency under coil misalignment," *IEEE Trans. Power Electron.*, vol. 30, no. 10, pp. 5632–5649, Oct. 2015.

[61] J. L. Villa, J. Sallan, J. F. S. Osorio, and A. Llombart, "High-misalignment tolerant compensation topology for ICPT systems," *IEEE Trans. Ind. Electron.*, vol. 59, no. 2, pp. 945–951, Feb. 2012.

[62] M. J. Chabalko and A. P. Sample, "Three-dimensional charging via multimode resonant cavity enabled wireless power transfer," *IEEE Trans. Power Electron.*, vol. 30, no. 11, pp. 6163–6173, Nov. 2015.

[63] B. H. Choi, E. S. Lee, Y. H. Sohn, G. C. Jang, and C. T. Rim, "Six degrees of freedom mobile inductive power transfer by crossed dipole Tx and Rx coils," *IEEE Trans. Power Electron.*, vol. 31, no. 4, pp. 3252–3272, Apr. 2016.

[64] E. S. Lee, J. S. Choi, H. S. Son, S. H. Han, and C. T. Rim, "Six degrees of freedom wide-range ubiquitous IPT for IoT by DQ magnetic field," *IEEE Trans. Power Electron.*, vol. 32, no. 11, pp. 8258–8276, Nov. 2017.

[65] C. Zhang, D. Lin, and S. Y. Hui, "Basic control principles of omnidirectional wireless power transfer," *IEEE Trans. Power Electron.*, vol. 31, no. 7, pp. 5215–5227, Jul. 2016.

[66] D. Lin, C. Zhang, and S. Y. R. Hui, "Mathematical analysis of omnidirectional wireless power transfer – Part I: Two-dimensional systems," *IEEE Trans. Power Electron.*, vol. 32, no. 1, pp. 625–633, Jan. 2017.

[67] D. Lin, C. Zhang, and S. Y. R. Hui, "Power and efficiency of 2-D omnidirectional wireless power transfer systems," in *Proc. IEEE Energy Convers. Congr. Expo.*, Montreal, QC, Canada, 2015, pp. 4951–4958.

[68] B. Che, F. Meng, and Q. Wu, "An omnidirectional wireless power transmission system with controllable magnetic field distribution," in *Proc. IEEE Int. Workshop Electromagn., Appl. Student Innov. Competition*, Nanjing, China, 2016, pp. 1–3.

[69] N. Ha-Van and C. Seo, "Analytical and experimental investigations of omnidirectional wireless power transfer using a cubic transmitter," *IEEE Trans. Ind. Electron.*, vol. 65, no. 2, pp. 1358–1366, Feb. 2018.

[70] D. Lin, C. Zhang, and S. Y. R. Hui, "Mathematic analysis of omnidirectional wireless power transfer – Part II three-dimensional systems," *IEEE Trans. Power Electron.*, vol. 32, no. 1, pp. 613–624, Jan. 2017.

[71] C. Zhang, D. Lin, and S. Y. R. Hui, "Omni-directional wireless power transfer systems using discrete magnetic field vector control," in *Proc. IEEE Energy Convers. Congr. Expo.*, Montreal, QC, Canada, 2015, pp. 3203–3208.

[72] Z. Zhang, K. T. Chau, C. Qiu, and C. Liu, "Energy encryption for wireless power transfer," *IEEE Trans. Power Electron.*, vol. 30, no. 9, pp. 5237–5246, Sep. 2015.

[73] Z. Zhang, K. T. Chau, C. Liu, C. Qiu, and F. Lin, "An efficient wireless power transfer system with security considerations for electric vehicle applications," *J. Appl. Phys.*, vol. 115, no. 17, pp. 17A328:1–3, 2014.

[74] A. Alphones and J. P. K. Sampath, "Metamaterial assisted wireless power transfer system," in *Proc. Asia-Pac. Microw. Conf.*, Nanjing, China, 2015, pp. 1–3.

[75] F. Bilotti and L. Sevgi, "Metamaterials: Definitions, properties, applications, and FDTD-based modeling and simulation," *Int. J. RF Microw. Comput. Aided Eng.*, vol. 22, no. 4, pp. 422–438, 2012.

[76] K. Y. Kim, "Comparative analysis of guided modal properties of double-positive and double-negative metamaterial slab waveguides," *Radioengineering*, vol. 18, no. 2, pp. 117–123, 2009.

[77] Y. Cho *et al.*, "Hybrid metamaterial with zero and negative permeability to enhance efficiency in wireless power transfer system," in *Proc. IEEE Wireless Power Transfer Conf.*, Aveiro, Portugal, 2016, pp. 1–3.

[78] B. Wang, K. H. Teo, T. Nishino, W. Yerazunis, J. Barnwell, and J. Zhang, "Wireless power transfer with metamaterials," in *Proc. 5th Eur. Conf. Antennas Propag.*, Rome, Italy, 2011, pp. 3905–3908.

[79] B. Wang and K. H. Teo, "Metamaterials for wireless power transfer," in *Proc. IEEE Int. Workshop Antenna Technol.*, Tucson, AZ, USA, 2012, pp. 161–164.

[80] Y. Dong, W. Li, W. Cai, C. Yao, D. Ma, and H. Tang, "Experimental investigation of 6.78 MHz metamaterials for efficiency enhancement of wireless power transfer system," in *Proc. IEEE 2nd Annu. Southern Power Electron. Conf.*, Auckland, New Zealand, 2016, pp. 1–5.

[81] W. Li, P. Wang, C. Yao, Y. Zhang, and H. Tang, "Experimental investigation of 1D, 2D, and 3D metamaterials for efficiency enhancement in a 6.78 MHz wireless power transfer system," in *Proc. IEEE Wireless Power Transfer Conf.*, Aveiro, Portugal, 2016, pp. 1–4.

[82] A. Ranaweera, T. P. Duong, B. S. Lee, and J. K. Lee, "Experimental investigation of 3D metamaterial for mid-range wireless power transfer," in *Proc. IEEE Wireless Power Transfer Conf.*, Jeju, South Korea, 2014, pp. 92–95.

[83] J. Choi and C. H. Seo, "High-efficiency wireless energy transmission using magnetic resonance based on negative refractive index metamaterial," *Prog. Electromagn. Res.*, vol. 106, pp. 33–47, 2010.

[84] J. Wu, B. Wang, W. S. Yerazunis, and K. H. Teo, "Wireless power transfer with artificial magnetic conductors," in *Proc. IEEE Wireless Power Transfer Conf.*, Perugia, Italy, 2013, pp. 155–158.

[85] A. Ranaweer, C. A. Moscoso, and J. W. Lee, "Anisotropic metamaterial for efficiency enhancement of mid-range wireless power transfer under coil misalignment," *J. Phys. D, Appl. Phys.*, vol. 48, no. 45, pp. 455104:1–8, 2015.

[86] B. Wang, W. Yerazunis, and K. H. Teo, "Wireless power transfer: Metamaterials and array of coupled resonators," *Proc. IEEE*, vol. 101, no. 6, pp. 1359–1368, Jun. 2013.

[87] W. Yerazunis, B. Wang, and K. H. Teo, "Metamaterials and resonant array wireless power systems," in *Proc. IEEE Antennas Propag. Soc. Int. Symp.*, Memphis, TN, USA, 2014, pp. 1403–1404.

[88] C. C. Mi, G. Buja, S. Y. Choi, and C. T. Rim, "Modern advances in wireless power transfer systems for roadway powered electric vehicles," *IEEE Trans. Ind. Electron.*, vol. 63, no. 10, pp. 6533–6545, Oct. 2016.

[89] J. Dai and D. C. Ludois, "Capacitive power transfer through a conformal bumper for electric vehicle charging," *IEEE J. Emerg. Sel. Topics Power Electron.*, vol. 4, no. 3, pp. 1015–1025, Sep. 2016.

[90] F. Lu, H. Zhang, and C. Mi, "A two-plate capacitive wireless power transfer system for electric vehicle charging applications," *IEEE Trans. Power Electron.*, vol. 33, no. 2, pp. 964–969, Feb. 2018.
[91] S. Li, Z. Liu, H. Zhao, L. Zhu, and Z. Chen, "Wireless power transfer by electric field resonance and its application in dynamic charging," *IEEE Trans. Ind. Electron.*, vol. 63, no. 10, pp. 6602–6612, Oct. 2016.
[92] S. Li and C. C. Mi, "Wireless power transfer for electric vehicle applications," *IEEE J. Emerg. Sel. Topics Power Electron.*, vol. 3, no. 1, pp. 4–17, Mar. 2015.
[93] C. S. Wang, O. H. Stielau, and G. A. Covic, "Design considerations for a contactless electric vehicle battery charger," *IEEE Trans. Ind. Electron.*, vol. 52, no. 5, pp. 1308–1314, Oct. 2005.
[94] W. Zhang, J. C. White, A. M. Abraham, and C. C. Mi, "Loosely coupled transformer structure and interoperability study for EV wireless charging systems," *IEEE Trans. Power Electron.*, vol. 30, no. 11, pp. 6356–6367, Nov. 2015.
[95] M. Budhia, G. A. Covic, and J. T. Boys, "Design and optimization of circular magnetic structures for lumped inductive power transfer systems," *IEEE Trans. Power Electron.*, vol. 26, no. 11, pp. 3096–3108, Nov. 2011.
[96] M. Budhia, J. T. Boys, G. A. Covic, and H. Chang-Yu, "Development of a single-sided flux magnetic coupler for electric vehicle IPT charging systems," *IEEE Trans. Ind. Electron.*, vol. 60, no. 1, pp. 318–328, Jan. 2013.
[97] S. Y. Choi, J. Huh, W. Y. Lee, and C. T. Rim, "Asymmetric coil sets for wireless stationary EV chargers with large lateral tolerance by dominant field analysis," *IEEE Trans. Power Electron.*, vol. 29, no. 12, pp. 6406–6420, Dec. 2014.
[98] Z. Zhang and K. T. Chau, "Homogeneous wireless power transfer for move-and-charge," *IEEE Trans. Power Electron.*, vol. 30, no. 11, pp. 6213–6220, Nov. 2015.
[99] A. Zaheer, G. A. Covic, and D. Kacprzak, "A bipolar pad in a 10-kHz 300-W distributed IPT system for AGV applications," *IEEE Trans. Ind. Electron.*, vol. 61, no. 7, pp. 3288–3301, Jul. 2014.
[100] G. A. Covic, M. L. G. Kissin, D. Kacprzak, N. Clausen, and H. Hao, "A bipolar primary pad topology for EV stationary charging and highway power by inductive coupling," in *Proc. IEEE Energy Convers. Congr. Expo.*, 2011, pp. 1832–1838.
[101] A. Zaheer, D. Kacprzak, and G. A. Covic, "A bipolar receiver pad in a lumped IPT system for electric vehicle charging applications," in *Proc. IEEE Energy Convers. Congr. Expo.*, 2012, pp. 283–290.
[102] S. W. Lee, J. Huh, C. B. Park, N. S. Choi, G. H. Cho, and C. T. Rim, "On-line electric vehicle using inductive power transfer system," in *Proc. IEEE Energy Convers. Congr. Expo.*, 2010, pp. 1598–1601.
[103] G. A. J. Elliott, G. A. Covic, D. Kacprzak, and J. T. Boys, "A new concept: Asymmetrical pick-ups for inductively coupled power transfer monorail systems," *IEEE Trans. Magn.*, vol. 42, no. 10, pp. 3389–3391, Oct. 2006.
[104] J. Huh, S. W. Lee, W. Y. Lee, G. H. Cho, and C. T. Rim, "Narrow-width inductive power transfer system for online electrical vehicles," *IEEE Trans. Power Electron.*, vol. 26, no. 12, pp. 3666–3679, Dec. 2011.
[105] S. Y. Choi, S. Y. Jeong, B. W. Gu, G. C. Lim, and C. T. Rim, "Ultraslim S-type power supply rails for roadway-powered electric vehicles," *IEEE Trans. Power Electron.*, vol. 30, no. 11, pp. 6456–6468, Nov. 2015.
[106] A. Khaligh and S. Dusmez, "Comprehensive topological analysis of conductive and inductive charging solutions for plug-in electric vehicles," *IEEE Trans. Veh. Technol.*, vol. 61, no. 8, pp. 3475–3489, Oct. 2012.
[107] M. Borage, S. Tiwari, and S. Kotaiah, "Analysis and design of an LCL-T resonant converter as a constant-current power supply," *IEEE Trans. Ind. Electron.*, vol. 52, no. 6, pp. 1547–1554, Dec. 2005.
[108] C. Liu, S. Ge, Y. Guo, H. Li, and G. Cai, "Double-LCL resonant compensation network for electric vehicles wireless power transfer: Experimental study and analysis," *IET Power Electron.*, vol. 9, no. 11, pp. 2262–2270, 2016.
[109] F. Lu, H. Zhang, H. Hofmann, and C. Mi, "A double-sided LCLC-compensated capacitive power transfer system for electric vehicle charging," *IEEE Trans. Power Electron.*, vol. 30, no. 11, pp. 6011–6014, Nov. 2015.
[110] S. Li, W. Li, J. Deng, T. D. Nguyen, and C. C. Mi, "A double-sided LCC compensation network and its tuning method for wireless power transfer," *IEEE Trans. Veh. Technol.*, vol. 64, no. 6, pp. 2261–2273, Jun. 2015.
[111] W. Li, H. Zhao, S. Li, J. Deng, T. Kan, and C. C. Mi, "Integrated LCC compensation topology for wireless charger in electric and plug-in electric vehicles," *IEEE Trans. Ind. Electron.*, vol. 62, no. 7, pp. 4215–4225, Jul. 2015.
[112] H. Feng, T. Cai, S. Duan, J. Zhao, X. Zhang, and C. Chen, "An LCC compensated resonant converter optimized for robust reaction to large coupling variation in dynamic wireless power transfer," *IEEE Trans. Ind. Electron.*, vol. 63, no. 10, pp. 6591–6601, Oct. 2016.
[113] J. M. Miller, O. C. Onar, and M. Chinthavali, "Primary-side power flow control of wireless power transfer for electric vehicle charging," *IEEE J. Emerg. Sel. Topics Power Electron.*, vol. 3, no. 1, pp. 147–162, Mar. 2015.
[114] H. H. Wu, A. Gilchrist, K. D. Sealy, and D. Bronson, "A high efficiency 5 kW inductive charger for EVs using dual side control," *IEEE Trans. Ind. Informat.*, vol. 8, no. 3, pp. 585–595, Aug. 2012.
[115] T. Diekhans and R. W. D. Doncker, "A dual-side controlled inductive power transfer system optimized for large coupling factor variations and partial load," *IEEE Trans. Power Electron.*, vol. 30, no. 11, pp. 6320–6328, Nov. 2015.
[116] U. K. Madawala and D. J. Thrimawithana, "A bidirectional inductive power interface for electric vehicles in V2G systems," *IEEE Trans. Ind. Electron.*, vol. 58, no. 10, pp. 4789–4796, Oct. 2011.
[117] J. S. Ho, K. Sanghoek, and A. Y. Poon, "Midfield wireless powering for implantable systems," *Proc. IEEE*, vol. 101, no. 6, pp. 1369–1378, Jun. 2013.
[118] M. R. Basar, M. Y. Ahmad, J. Cho, and F. Ibrahim, "Stable and high-efficiency wireless power transfer system for robotic capsule using a modified Helmholtz coil," *IEEE Trans. Ind. Electron.*, vol. 64, no. 2, pp. 1113–1122, Feb. 2017.
[119] H. Liu, Q. Shao, and X. Fang, "Modeling and optimization of class-E amplifier at subnominal condition in a wireless power transfer system for biomedical implants," *IEEE Trans. Biomed. Circuits Syst.*, vol. 11, no. 1, pp. 35–43, Feb. 2017.
[120] A. Ibrahim and M. Kiani, "A figure-of-merit for design and optimization of inductive power transmission links for millimeter-sized biomedical implants," *IEEE Trans. Biomed. Circuits Syst.*, vol. 10, no. 6, pp. 1100–1111, Dec. 2016.
[121] B. Lee, M. Kiani, and M. Ghovanloo, "A triple-loop inductive power transmission system for biomedical applications," *IEEE Trans. Biomed. Circuits Syst.*, vol. 10, no. 1, pp. 138–48, Feb. 2016.
[122] S. Ping, A. P. Hu, S. Malpas, and D. Budgett, "A frequency control method for regulating wireless power to implantable devices," *IEEE Trans. Biomed. Circuits Syst.*, vol. 2, no. 1, pp. 22–29, Mar. 2008.
[123] A. Dukju and H. Songcheol, "Wireless power transmission with self-regulated output voltage for biomedical implant," *IEEE Trans. Ind. Electron.*, vol. 61, no. 5, pp. 2225–2235, May 2014.
[124] S. A. Mirbozorgi, P. Yeon, and M. Ghovanloo, "Robust wireless power transmission to mm-sized free-floating distributed implants," *IEEE Trans. Biomed. Circuits Syst.*, vol. 11, no. 3, pp. 692–702, Jun. 2017.
[125] T. Sun, X. Xie, G. Li, Y. Gu, Y. Deng, and Z. Wang, "A two-hop wireless power transfer system with an efficiency-enhanced power receiver for motion-free capsule endoscopy inspection," *IEEE Trans. Biomed. Eng.*, vol. 59, no. 11, pp. 3247–3254, Nov. 2012.
[126] S. C. Tang, T. L. T. Lun, Z. Guo, K. W. Kwok, and N. J. McDannold, "Intermediate range wireless power transfer with segmented coil transmitters for implantable heart pumps," *IEEE Trans. Power Electron.*, vol. 32, no. 5, pp. 3844–3857, May 2017.

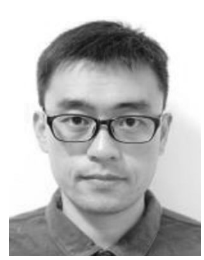

Zhen Zhang (S'11–M'13–SM'15) received the B.Eng. and M.Eng. degrees from Tianjin University, Tianjin, China, in 2004 and 2007, respectively, and the Ph.D. degree from The University of Hong Kong, Hong Kong, in 2014, all in electrical engineering.

In 2014, he took a short-term visiting at IBM Research—China, supported by the IBM Global Great Minds Program. Then, he served as a Postdoctoral Fellow with The University of Hong Kong. He is currently an Associate Professor with the School of Electrical and Information Engineering, Tianjin University. He has authored or coauthored more than 30 internationally refereed papers and one sole-authored book published by the Cambridge University Press. His research interests include wireless power transfer, electric drives, electric vehicles, power electronics, and distributed energies.

Dr. Zhang is currently an Associate Editor for the IEEE TRANSACTIONS ON INDUSTRIAL ELECTRONICS, Associated Editor for the IEEE TRANSACTIONS ON INDUSTRIAL INFORMATICS, Editor for the IEEE TRANSACTIONS ON MAGNETICS, Associate Editor for *IET Renewable Power Generation*, and Executive Editor of Cambridge University—Wireless Power Transfer.

Hongliang Pang (S'17) was born in Tianjin, China. He received the B.Eng. degree in automation in 2017 from Tianjin University, Tianjin, China, where he is currently working toward the M.S. degree in control science and engineering.

His current research interests include wireless power transfer and power-electronic-based impedance matching.

Apostolos Georgiadis (S'94–M'02–SM'08) was born in Thessaloniki, Greece. He received the B.S. degree in physics and the M.S. degree in telecommunications from the Aristotle University of Thessaloniki, Thessaloniki, Greece, in 1993 and 1996, respectively, and received the Ph.D. degree in electrical engineering from the University of Massachusetts, Amherst, MA, USA, in 2002.

In 1995, he spent a semester with Radio Antenna Communications, Milan, Italy, working on Yagi antennas for U.H.F. applications. In 2002, he joined Global Communications Devices, North Andover, MA, USA, as a Systems Engineer and worked on CMOS transceivers for wireless network applications. In June 2003, he joined Bermai, Inc., Minnetonka, MN, USA, as an RF/Analog Systems Architect. In 2005, he joined the University of Cantabria, Spain, as a Juan de la Cierva Fellow Researcher. In March 2007, he joined CTTC, Spain, as a Senior Research Associate working in the area of communications subsystems. During 2013–2016, he was the Group Leader of the Microwave Systems and Nanotechnology Department, CTTC. In July 2016, he joined Heriot-Watt University as an Associate Professor, and currently holds an Honorary Associate Professor position. He has authored or coauthored more than 180 papers in peer-reviewed journals and international conferences. His research interests include energy harvesting and wireless power transmission, RFID technology, active antennas and phased array antennas, inkjet and three-dimensional printed electronics, and millimeter wave systems.

Dr. Georgiadis was the recipient of the Fulbright Scholarship for graduate studies from the University of Massachusetts, in 1996. He was the General Chair of 2011 IEEE RFID-TA Conference, and General Cochair of the 2011 IEEE MTT-S IMWS on Millimeter Wave Integration Technologies. He is member of the IEEE MTT-S TC-24 RFID Technologies (past Chair) and member of IEEE MTT-S TC-26 Wireless Energy Transfer and Conversion. He serves as an Associate Editor of the IEEE JOURNAL ON RFID. He has been Associate Editor for the IEEE MICROWAVE AND WIRELESS COMPONENTS LETTERS, the *IET Microwaves Antennas and Propagation*, and the IEEE RFID VIRTUAL JOURNAL. He cofounded and was the Editor-in-Chief of the *Cambridge Wireless Power Transfer Journal*. He has been a Distinguished Lecturer of IEEE CRFID. He is an EU Marie Curie Global Fellow. He is Chair of URSI Commission D: Electronics and Photonics.

Carlo Cecati (M'90–SM'03–F'06) received the Dr.Ing. degree in electrotechnical engineering from the University of L'Aquila, L'Aquila, Italy, in 1983.

Since 1983, he has been with the University of L'Aquila, where since 2006, he has been a Professor of Industrial Electronics and Drives with the Department of Information Engineering, Computer Science, and Mathematics. From 2015 till September 2017, he was a Qianren Talents Professor (1000 Talents Program Distinguished Professor) with the Harbin Institute of Technology, Harbin, China. His research interests include power electronics, distributed generation, and smart grids. In these fields, he has authored more than 180 journal and conference papers.

Prof. Cecati has been an active member of the IEEE Industrial Electronics Society since 1990 and he has been a Senior AdCom Member since 2006. From 2013 to 2015, he was the Editor-in-Chief for the IEEE TRANSACTIONS ON INDUSTRIAL ELECTRONICS. He was the recipient of the 2012 and 2013 Best Paper Awards from the IEEE TRANSACTIONS ON INDUSTRIAL INFORMATICS, and the 2012 Best Paper Award from the *IEEE Industrial Electronics Magazine*.